An estimator for the Coulomb repulsion parameter U to generate vacuum referred binding energy schemes for lanthanides in compounds

Dorenbos, Pieter

Important note
To cite this publication, please use the final published version (if applicable).
Please check the document version above.

Full Length Article

An estimator for the Coulomb repulsion parameter U to generate vacuum referred binding energy schemes for lanthanides in compounds

Pieter Dorenbos

Delft University of Technology, Faculty of Applied Sciences, Department of Radiation Science and Technology, Mekelweg 15, 2629 JB Delft, Netherlands

ARTICLE INFO

ABSTRACT

The U-value defined as the energy difference between the $Eu^{4+/3+}$ and $Eu^{3+/2+}$ charge transition levels (CTLs) is the most important parameter in constructing vacuum referred binding energy diagrams (VRBEs) with all the lanthanide CTLs with respect to the vacuum level of energy. The parameter is difficult to determine from experiment and the aim of this work is to establish a method to estimate the U-value from the average electronegativity of the cations in the compound. Since the U-value is controlled by the same physical processes, i.e., covalence and anion polarizability, as the centroid shift ϵ_c of the Ce^{3+} 5d configuration, one may estimate the U-value from that centroid shift. That method provides already good values for U for about 175 different compounds. Those U-values are compared with the average cation electronegativity χ_{av}, and relations will be established from which the U-value can be estimated with about ± 0.1 eV accuracy from just the composition of the compound. It can be applied to all types of stoichiometric inorganic compounds like the halides (F, Cl, Br, I), chalcogenides (O, S, Se), and nitrides (N). The U-value complemented with the bandgap and the energy needed for electron transfer from the valence band top to a trivalent lanthanide dopant is then sufficient to construct a VRBE diagram with all lanthanide levels with respect to the vacuum level and the host valence and conduction bands.

1. Introduction

The location of the lanthanide charge transition levels (CTLs) with respect to the host valence or conduction band controls many fascinating properties of lanthanide activated materials. It determines the preferred valence state (2+, 3+, 4+) of a lanthanide [1], it determines whether a lanthanide is a potential hole trapping or electron trapping center and also how deep those charge carrier traps are [2]. Luminescence quantum efficiency and thermal quenching temperature of lanthanide luminescence is often linked to electron transfer to the conduction band (CB) or hole transfer to the valence band (VB) and again CTL locations are crucial [3]. Catalytic activity of for example CeO_2 [4] is also directly related to the energy of the $Ce^{4+/3+}$ CTL with respect to the vacuum level.

Methods to construct host referred binding energy (HRBE) schemes with all $Ln^{3+/2+}$ and $Ln^{4+/3+}$ CTLs in the band gap have a history starting already around 1985 with the works of McClure and co-workers on the alkali earth fluoride compounds [5,6]. With photoconductivity studies, the $Ln^{3+/2+}$ CTLs were established with respect to the CB-bottom. Gradually other experimental techniques like photoelectron spectroscopy by Thiel et al. [7,8] providing the $Ln^{4+/3+}$ CTLs with respect to the valence band (VB) top and techniques like excited state absorption were added [9,10]. Yen et al. [11,12] used spectroscopic techniques to determine so-called charge transfer bands in excitation spectra of trivalent lanthanides to establish $Ln^{3+/2+}$ CTLs above the VB-top. In 2003 Dorenbos collected available information, and standardized the HRBE construction method [13]. In following years the method was applied to many compounds and verified with techniques like thermoluminescence [2,14]. Ten years later in 2012, the chemical shift model was developed that enabled to convert a HRBE scheme into a vacuum referred binding energy scheme (VRBE), and in addition a model was provided to explain level location quantitatively [16,17].

Fig. 1 shows an example VRBE diagram with the $Ln^{3+/2+}$ and $Ln^{4+/3+}$ CTLs. There are three main parameters plus five secondary parameters needed for scheme construction The main parameters are; i) the exciton creation energy E^{ex} (see arrow 1)), ii) the energy of electron transfer from the VB-top to one of the trivalent lanthanides ($E^{CT}(Ln^{3+})$) which is usually Eu^{3+} (see arrow 2), and iii) the energy difference between the $Eu^{4+/3+}$ and $Eu^{3+/2+}$ CTLs which is known as the U-value (see arrow 3). In addition, we need the exciton binding energy E_{e-h}
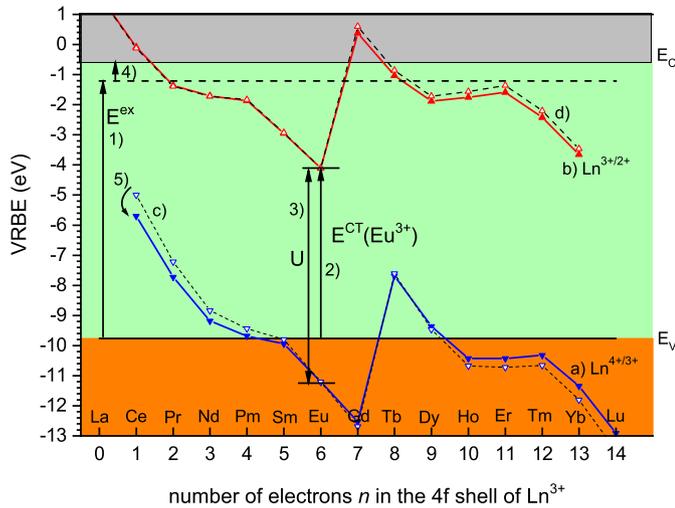
Fig. 1. A vacuum referred binding energy diagram obtained with $U = 7.09$ eV, $E^{ex} = 8.55$ eV, $E^{CT}(Eu^{3+}) = 5.65$ eV where the location of the $Ln^{3+/2+}$ and $Ln^{4+/3+}$ charge transition levels are connected with characteristic zigzag solid curves a) and b). The arrows 1), 2), and 3) indicate the three energies of the main parameters needed to construct the diagram. Curve c) shows the $Ln^{4+/3+}$ CTL curve when no correction ($\alpha(3+) = 0$) would be made for the lanthanide contraction, and curve d) shows the $Ln^{3+/2+}$ CTL curve when no correction ($\beta(2+) = 1$) would be made for the nephelauxetic effect.

(see arrow 4) to place the CB-bottom above the VB-top. Usually E_{e-h} is approximated as $0.008 \times (E^{ex})^2$ [15]. Curves a) and b) in Fig. 1 connect the $Ln^{4+/3+}$ and $Ln^{3+/2+}$ CTLs from La to Lu. These are derived from the 4th and 3rd ionization potentials of the lanthanides. By means of the contraction tilt parameters $\alpha(2+)$ and $\alpha(3+)$ a correction is made for the changing lanthanide ionic radius on CTL energy. The dashed curve c) in Fig. 1 connects the free lanthanide $Ln^{4+/3+}$ CTLs (equivalent to the negative of the 4th ionization potentials) shifted to coincide at the $Eu^{4+/3+}$ CTL in the diagram. Arrow 5) illustrates the tilting due to the $\alpha(3+)$ parameter. In 2019 a refinement on VRBE level location or CTLs was introduced that incorporates the nephelauxetic effect on the binding in $4f^n$ ground states [18,19]. This added the last two secondary parameters, i.e., the nephelauxetic parameters $\beta(2+)$ and $\beta(3+)$. The dashed curve d) connects the $Ln^{3+/2+}$ CTLs when such correction is not applied. It demonstrates that the correction is only significant for the lanthanides with more than half filled 4f-orbital. The α and β parameters do not depend strongly on type of compound and they can be estimated from the U-value. One therefore needs only the three main parameters to construct a VRBE diagram with all lanthanide CTLs with respect to the vacuum level and with respect to the host bands.

The $U(A)$-value for the chemical environment A is the most crucial parameter. In the chemical shift model a relationship between $U(A)$ and the Eu CTLs was established [18]

$$CTL(Eu^{3+/2+}, A) = -24.92 + \frac{18.05 - U(A)}{0.777 - 0.0353 U(A)} \quad (1)$$

and

$$CTL(Eu^{4+/3+}, A) = CTL(Eu^{3+/2+}, A) - U(A) \quad (2)$$

where the last term in Eq. (1) is the chemical shift $E_{cs}(Eu^{2+})$ of the $Eu^{3+/2+}$ CTL in compound A and 24.92 eV is the third ionization potential of Eu [16].

In principle the value for $U(A)$ can be derived when experimental data on the energy for charge carrier transfer from several different lanthanides to the host bands are combined in a HRBE diagram. One may think of 1) the energy to transfer an electron from the VB-top to a trivalent lanthanide (CT-bands), 2) the energy to transfer an electron from a trivalent lanthanide to the CB-bottom (Intervalence CT bands), 3) the transfer of an electron from an excited lanthanide state to the CB

(thermal quenching energy barriers), 4) the energy needed to de-trap an electron from a lanthanide to the CB as determined by thermoluminescence techniques (electron capture and de-trapping), 5) the energy needed to de-trap a hole from a lanthanide to the valence band (hole capture and de-trapping). All this information collected in one diagram together with the well-established $Ln^{3+/2+}$ and $Ln^{4+/3+}$ CTL curve shapes provides the HRBE diagram from which the $U(A)$ value can be read from. The diagram can then be converted into a VRBE diagram with Eq. (1).

It was soon found that the $U(A)$ value scales with how strong electrons are bonded in the anion ligands that surround the lanthanide, in this case Eu, in the compound. The value is lowest for the pure lanthanide metals with freely moving conduction band electrons and largest in fluoride compounds where electrons are strongly bonded in the fluorine [16,20].

This work will first review the methods on how to determine the U-value for a compound. The method based on constructed HRBE diagrams requires many pieces of information involving different lanthanides in the same compound. Another method is based on the centroid shift of the Ce^{3+} 5d-levels. That method will be applied to a set of 175 different compounds. The U-values of those 175 compounds will form a basis to generate estimation tools for the U-value based on the electronegativity values of the cations in the compound. It is the aim of this work to arrive at an estimation tool that generates $U(A)$-values for countless different types of inorganic compounds. Just the knowledge on the stoichiometric compostion of a compound will then be sufficient to generate all lanthanide CTLs for that compound. This together with the bandgap of the material and one experimentally determined $E^{CT}(Ln^{3+})$ value, that are already known for at least 1000 different compounds, will be sufficient to generate the VRBE schemes for all those compounds.

2. Historic developments to determine the U-value for Eu

Let us first address the $U(A)$-value when the environment A is just vacuum which is the situation for the lanthanides in the gas phase. The fourth ionization potential of Eu atoms is 42.97 eV which translates to a VRBE of -42.97 eV for the $Eu^{4+/3+}$ CTL with the $4f^6$ electron configuration. Let us now add an electron into the 4f-shell to obtain Eu^{2+}. Coulomb repulsion with the other 4f-electrons reduces the binding energy with 18.05 eV to obtain the $Eu^{3+/2+}$ CTL at -24.93 eV equivalent to the third ionization potential of Eu. For that reason the U-value is named the Coulomb repulsion energy.

In [20], U-values of about 40 different inorganic compounds and of pure Eu metal were compiled. These values were read from constructed HRBE schemes. There appears a relation between the U-value and the centroid shift of Ce^{3+} 5d-levels. The 5d excited states of Ce^{3+} in compounds are subject to a crystal field splitting into at most five distinct states. In addition, the average energy of the five 5d-states above the $4f^1$ ground state is shifted towards lower energy as compared to the free ion value of 6.35 eV. This centroid shift energy $\epsilon_c(A)$, like the $U(A)$-value, appears to be related to how strong electrons are bonded in the anion ligands that surround Ce^{3+} as was demonstrated in [21]. The shift is due to covalence between the 5d-orbitals and the surrounding anion ligands and also due to a correlated motion between the 5d-electron and the electrons in the anion ligands. Both contributions are related to the electronic polarizability of the anion ligands and therefore with how strong the ligands are bonded. Since the U-value and the centroid shift are determined by similar physical and chemical interactions between the lanthanide and surrounding anions, a relation between both is to be expected. This was further analyzed in [20] where the data on the U-value of the 40 different compounds were compared with data on the Ce^{3+} centroid shift in the same set of compounds. Results are reproduced in Fig. 2.
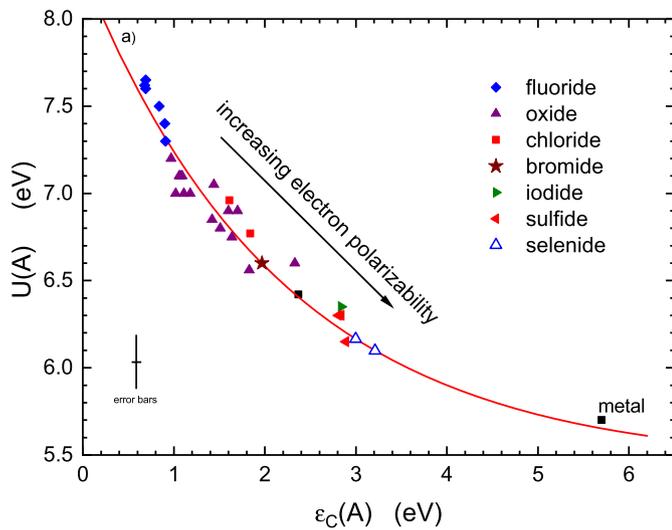
Fig. 2. $U(A)$ as derived from HRBE schemes shown as function of the centroid shift as derived from Ce^{3+} spectroscopy. Solid line a) shows the empirical relation between both. Data from [22] were used.

A solid curve given by the entirely empirical relation

$$U_c(A) = 5.44 + 2.834e^{-\epsilon_c(A)/2.2} \tag{3}$$

is running through the data in Fig. 2. Here the subscript c is introduced to indicate that the U-value is obtained from the centroid shift. The U-value determined from a HRBE scheme has typically ± 0.15 eV error. The centroid shift is much easier to obtain with only ± 0.05 eV error and is well-established for many different compounds. That of 150 compounds were compiled in [22], and in the mean time values on 25 more compounds became available. One may now use the value for the centroid shift as an estimator for the U_c-value by utilizing Eq. (3) as was done in [20,22]. In principle this generates U_c-values for 175 different compounds. However, for most compounds, particularly those where Ce^{3+} does not luminescence or where more than one possible Ce^{3+} site is present, it is difficult or impossible to measure or assign all five 4f-5d transitions needed to derive the centroid shift.

The challenge is now to find a good estimator for the U-value for compounds for which the centroid shift is not available. For that we will use the ideas and theory behind the centroid shift value as outlined in [21]. In that work the concept of spectroscopic polarizablility α_{sp} was introduced, a parameter closely tied to the polarizability of the anion ligands that is related to the centroid shift ϵ_c as [23,24]

$$\frac{1}{\alpha_{sp}} = \frac{1.79 \times 10^{13}}{\epsilon_c} \sum_{i=1}^{N} \frac{1}{(R_i - f\Delta R)^6} \tag{4}$$

where ϵ_c is in eV, bondlengths R_i in pm, and α_{sp} in units of 10^{30} m^{-3}. The summation is over the N coordinating anions located a distance R_i from Ce^{3+}. ΔR is the difference between the ionic radius of Ce^{3+} with the ionic radius of the cation it substitutes for. Ionic radii can be obtained from the tabulations by Shannon [25]. The relaxation fraction f is introduced to account for lattice relaxation around Ce^{3+}. The value of f is chosen 0.6 for all N ligands. With Eq. (4) and crystallographic data on the compound, the observed centroid shift can be translated into the value for α_{sp}. Next, a linear relationship between the thus obtained α_{sp} and the average electronegativity χ_{av} of the cations in the compound was demonstrated

$$\alpha_{sp} = a(X) + \frac{b(X)}{\chi_{av}^2} \tag{5}$$

where $a(X)$ is a constant that depends on anion X. $b(X)$ is a constant expressing the susceptibility of anion X to change its polarizability due to

bonding with coordinating cations. χ_{av} is the average electronegativity of the cations in the compound defined as

$$\chi_{av} = \frac{1}{\gamma N_a} \sum_{i}^{N_c} z_i \chi_i \tag{6}$$

where the summation runs over all cations N_c in the stoichiometric formula of the compound and where each cation with electronegativity χ_i is weighted with its formal charge z_i. N_a is the number of anions in the stoichiometric formula each with formal charge $-\gamma$. For example, in YPO_4 we deal with one cation Y with $z_i = 3$, one cation P with $z_i = 5$ and 4 anions O with $\gamma = 2$. There are many different types of electronegativity scales [27] but the Pauling scale is most common. The corrected Pauling values from the work by Allred [28] are reproduced in Fig. 3. For the cations Hf, Nb, Ta, Mo, and W, the original Pauling values [29] are used. With these cation electronegativity values the linear relationships were observed for the fluorides and oxides in [21] and later also for the nitrides in [26]. This implies that the centroid shift and then also the U-value can be predicted from the electronegativities of the cations in the compound and the Ce-anion bondlenghts in the lattice.

3. Proposed estimator method for the U-value

In principle one might follow the route to first compute χ_{av} from the stoichiometric composition of the compound and next α_{sp} with Eq. (5) using the constants for $a(X)$ and b(X) that were found in [21]. Using Eq. (4) and crystallographic information on the bondlengths, the centroid shift ϵ_c is obtained and from there the U_c-value. However, there are many pitfalls. When coordination around Ce^{3+} is very irregular it may become difficult to decide which ligands should be counted in the summation. Also for Ce^{3+} on large lattice sites like that of Ba^{2+} the lattice relaxation around Ce^{3+} may be such that the relaxation fraction f in Eq. (4) is not the same for each bond whereas a constant value is assumed. We aim to arrive at a more simple estimator. We will use the U_c-values computed from the centroid shift of the 150 different compounds in [22]. More data have become available that are compiled in Table 1. Table 1 also lists some revised values on the compounds of [22].

3.1. U-value estimator for oxide compounds

Fig. 4 shows the U_c-value for the oxide compounds against the average χ_{av} obtained with Eq. (6) using the electronegativities from Fig. 3. The data tend to fall in the shaded region in the figure that has a width of ± 0.1 eV. The solid curve through the shaded area is given by the polynomal

$$U_X^O = 4.79 + 1.9\chi_{av} - 0.33\chi_{av}^2 \tag{7}$$

that can be used as a first estimator for the U_X-value for oxides. The subscript X is used to indicate that the U-value is estimated from the average electronegativity.

There are several outlier data points. In each case this signals there is something wrong in the assignment of the five 4f-5d transitions or that somehow the method fails. The data on $BaSiO_3$, $SrSiO_3$, and Sr_2SiO_4 that were all obtained from [30] are not considered very reliable and need further confirmation. The same applies to LuP_3O_9 where the U_c-value from the centroid shift appears 0.3 eV smaller than U_X^O. Most likely the assignment in [22] of a weak 210 nm band observed in [31] to the fifth 4f-5d transition is not correct. Such wrong assignment is easily made knowing that there are four different Lu-sites in the lattice. For Ce^{3+} in the similar compound YP_3O_9, the fifth band was observed at 184 nm as listed in Table 1 resulting in a U_c-value in reasonable agreement with the predicted one. Also for $SrZn_2(PO_4)_2$ and SrB_2O_4 dedicated studies are needed to determine the centroid shift more reliably. Another deviating case is $Y_2O_2SO_4$ where U_c appears 0.4 eV

Fig. 3. The corrected Pauling electronegativities of atoms as compiled in [28]. For Hf, Nb, Ta, Mo, and W the orignal values from [29] were used.

Fig. 4. $U_c(A)$ as calculated from the centroid shift against $\chi_{av}(A)$ for the oxide compounds.

Fig. 5. $U_c(A)$ as calculated from the centroid shift against $\chi_{av}(A)$. Most data points are labeled with the cations present in the composition. Sequences of similar compounds with changing cation site are connected with dotted line segments. The location of the data for oxide compounds are represented by the dashed curve a).

smaller than the expected U_X^O. Possibly the wavelength of the fifth 4f-5d transition was estimated wrongly in [22,32] but that can still not account for the 0.4 eV difference. Here probably the method itself is failing. We deal with oxygen ligands strongly bonded in the sulfate groups together with unbound oxygen ligands. Y^{3+} is coordinated by four of these unbound oxygen at relatively close distance that contribute much to the centroid shift plus four oxygen bonded in sulfate groups that have small contribution. In such cases with oxygen ligands with strongly different polarizabilities or ligand bonding, working with an average cation electronegativity may not provide a good estimator.

A closer inspection of the data in Fig. 4 shows that for the same χ_{av} the U_c-value for compounds with the relatively small sites provided by Ca^{2+}, Gd^{3+}, Y^{3+}, Lu^{3+}, and Sc^{3+} tend to be somewhat smaller than on larger La^{3+}, Sr^{2+}, and Ba^{2+} sites. This is particularly evident for $Li_4SrCa(SiO_4)_2$ where the centroid shift on the small Ca-site appears 0.13 eV larger than on the large Sr-site leading to 0.09 smaller U_c in Table 1 and in Fig. 4. It is all related to the R^{-6} dependence in Eq. (4). The increasingly smaller bondlength outweighs the larger average electronegativity, and centroid shift tends to increase with smaller site size. We have to conclude that the centroid shift, the U-value and there-

with also the $Ln^{3+/2+}$ and $Ln^{4+/3+}$ CTL energies in a VRBE diagram are site dependent. The same applies to different crystal phases of the same compound. As first estimator for the U-value, Eq. (7) can be used. Next, one can make a small correction of about -0.05 eV in case of small lattice sites and +0.05 eV for large lattice sites.

3.2. U-value estimator for single anion type non-oxide compounds

Fig. 5 shows the calculated U_c-values for all compounds containing one single type of anion (F, Cl, Br, I, O, S, Se, N) where we have information on the centroid shift. In order not to overcrowd the figure, the values for the oxide compounds are represented by the curve given by Eq. (7).

The fluorine ligand is very poorly polarizable leading to small centroid shifts and large values for U_c. Like for the oxide compounds, the U_c-value increases with larger χ_{av} and the U_c-value on large lattice sites

Table 1

The wavelengths λ_i (in nm) of the five 4f-5d$_i$ transitions for Ce$^{3}+$ in compound A where values within braces are tentatively assigned. The centroid shift $\epsilon_c(A)$ and Coulomb repulsion energy $U_c(A)$ calculated there from are in eV.

A	$\lambda_5, \lambda_4, \lambda_3, \lambda_2, \lambda_1$	$\epsilon_c(A)$	$U_c(A)$	Ref.
fluorides		–	–	
LiSrAlF$_6$	158, 171, 253, 268, 268	0.502	7.69	[34,35]
K$_2$YF$_5$	177, 204, 220, 285, 296	0.898	7.32	[36]
chlorides		–	–	
K$_2$LaCl$_5$	221, 239, 252, 313, 330	0.931	7.29	[37,38]
iodides		–	–	
Cs$_2$NaLaI$_6$	(275, 285), 370, (2x)395	2.65	6.29	[39]
Cs$_2$LiLaI$_6$	298, 310, 370, 400, 400	2.70	6.27	[40]
oxy-halides		–	–	
Ba$_5$(PO$_4$)$_3$F:(6h)	200, 213, 247, 267, 293	1.17	7.10	[41]
Sr$_5$(PO$_4$)$_3$F:(6h)	192, 211, 241, 264, 296	1.04	7.20	[41]
Ca$_2$BO$_3$Cl	209, 234, 260, 325, 344	1.67	6.77	[42,43]
Sr$_3$(Al$_2$O$_5$)Cl$_2$	(206), 243, 274, 306, 335	1.67	6.76	[44–46]
phosphates		–	–	
NaLaP$_4$O$_{12}$	199, 210, 222, 253, 294	0.984	7.25	[47]
LiLaP$_4$O$_{12}$	189, 220, 229, 241, 288	0.939	7.29	[48]
orth.-GdP$_3$O$_9$	192, 202, 231, 269, 294	0.994	7.24	[49]
YP$_3$O$_9$	184, 210, 235, 282, 300	1.06	7.19	[50,51]
LuP$_3$O$_9$	210, 222, 240, 285, 300	1.32	6.99	[31]
BaMgP$_2$O$_7$	196, 217, 229, 259, 273	1.00	7.24	[52]
SrMgP$_2$O$_7$	191, 217, 231, 263, 285	1.02	7.22	[53]
KSrPO$_4$	204, 215, 237, 270, 300	1.19	7.09	[54]
K$_3$La(PO$_4$)$_2$	181, 210, 246, 270, 310	1.16	7.11	[55,56]
K$_3$Gd(PO$_4$)$_2$	192, 211, 243, 286, 305	1.18	7.09	[56]
γ-Na$_3$Gd(PO$_4$)$_2$	200, 213, 250, 270, 310	1.24	7.05	[57]
K$_3$Y(PO$_4$)$_2$	191, 210, 242, 289, 304	1.17	7.10	[56]
Ca$_9$Y(PO$_4$)$_7$	203,225,245,260,288	1.20	7.08	[58]
silicates		–	–	
CaMgSi$_2$O$_6$	193, 214, 245, 290, 325	1.28	7.02	[59]
Sr$_2$MgSi$_2$O$_7$	200, 217, 244, 269, 326	1.27	7.03	[60]
BaY$_2$Si$_3$O$_{10}$	184, 215, 292, 316, 332	1.47	6.89	[61–64]
Ba$_2$SiO$_4$	213,228,245,300,326	1.50	6.87	[65,66]
Sr$_3$Mg(SiO$_4$)$_2$	206, 239, 250, 269, 332	1.45	6.90	[67]
Li$_4$SrCa(SiO$_4$)$_2$ (Sr-site)	215, 234, 248, 264, 286	1.34	6.98	[68]
Li$_4$SrCa(SiO$_4$)$_2$ (Ca-site)	≈180, ≈190, 322, 337, 357	1.47	6.89	[68]
aluminates		–	–	
Ca$_2$Al(AlSiO$_7$)	221, 228, 246, 281, 356	1.56	6.83	[69–71]
LaAlO$_3$	(3x)(247), (302), 317	1.74	6.72	[72–75]
Lu$_3$Al$_5$O$_{12}$	(206), 220, 229, 348, 448	1.67	6.76	[76–79]
sulfides		–	–	
CaS	(2x)(287), 439, (2x)458	2.98	6.17	[80]
simple selenides		–	–	
SrSe	(2x)308, 415, (2x)435	3.00	6.16	[81]
CaSe	(2x)330, 433, (2x)455	–	–	[80,81]
nitrides		–	–	
Sr$_2$Si$_5$N$_8$	(260, 278), 329, 392, 432	2.55	6.33	[82]
Ca$_2$Si$_5$N$_8$	(261, 288), 329, 370, 397	2.49	6.35	[82]
CaAlSiN$_3$	(259), 313, 370, 421, 483	2.83	6.22	[83,84]

provided by K$^+$, Ba^{2+}, Sr^{2+}, La^{3+} tend to be somewhat larger than on small sites provided by Y^{3+}, Lu^{3+}, and Ca^{2+}. This is also demonstrated in the series of compounds BaF$_2$, SrF$_2$, CaF$_2$ where χ_{av} increases but U_c decreases. Similar applies to LiSrAlF$_6$, LiCaAlF$_6$ and KMgF$_3$, NaMgF$_3$ as illustrated in Fig. 5. Again we can make a simple first estimator using the solid curve b) in Fig. 5 given by

$$U_X^F = 5.95 + 1.8\chi_{av} - 0.38\chi_{av}^2 \qquad (8)$$

In cases of small sites like Y or Lu the U_X-value will be chosen slightly (at most 0.1 eV) smaller and for large site like from Ba^{2+} at most 0.1 eV larger.

There is very little data on the Ce^{3+} centroid shift in nitride compounds because the relatively small band gap of nitride compounds does not allow to determine the energies of all five 4f-5d transitions. All data available pertain to siliconitrides. The ionic radius of F$^-$, O^{2-} and N^{3-} do not differ much but their polarizability strongly increases with the valence, and in the same sequence centroid shift increases and U_c-value decreases. For the fluorine and oxygen a clear increase of U_c with increase of χ_{av} is observed as expressed with Eq. (7) and (8). For

the nitrides a similar relationship is to be expected but the number of data is too low to verify that.

In the sequence F$^-$, Cl$^-$, Br$^-$, and I$^-$ the anion polarizability increases and that is reflected in larger Ce^{3+} centroid shift and increasingly smaller value for U_c. Fluorides fall between 7.25 eV and 7.7 eV increasing with χ_{av}. Such increase is not seen for the other halides where U_c appears almost constant with values around 6.65-6.8 eV for chlorides, 6.5-6.6 eV for bromides, and 6.2-6.4 eV for iodides with a slight tendency that the relatively small Y^{3+}, Lu^{3+} and Ca^{2+} have relatively low U_c-value. The few data on sulfide and selenide compounds fall between 6.1-6.3 eV. Apparently the type of cation does not have much effect on the bonding and polarizability of the already highly polarizable large anions Cl, Br, I, S, Se.

3.3. U-value estimator for mixed anion type of compounds

A final group of compounds are those that contain two types of anions like La$_3$F$_3$(Si$_3$O$_9$) and LaOBr. For the oxyfluorides, one may calculate the contribution to α_{sp} from the oxide and fluoride anion separately to estimate ϵ_c and U_c. In the case of La$_3$F$_3$(Si$_3$O$_9$) a value of $\epsilon_c = 1.04$ eV was calculated in excellent agreement with the experimental value of 1.00 eV [33]. For other mixed anion compounds one may work with a weighted average U_w value as first approximation. For example, U_c(LaOBr)= 6.4 eV as obtained from the reported centroid shift [22]. It may also be estimated from a weighted average $U_w = (U_c(\text{La}_2\text{O}_3) + U_c(\text{LaBr}_3))/2 = (6.45+6.59)/3 = 6.52$ eV. Similarly, $U_w(\text{La}_3\text{F}_3(\text{Si}_3\text{O}_9)) = (U_c(\text{LaF}_3) + U_X^O(\text{La}_2(\text{Si}_3\text{O}_9))/2$. With $U_c(\text{LaF}_3) = 7.51$ eV [22] and with Eq. (7) and $\chi_{av}(\text{La}_2(\text{Si}_3\text{O}_9))=1.267$ yielding $U_X^O(\text{La}_2(\text{Si}_3\text{O}_9)) = 6.67$ eV one obtains $U_w(\text{La}_3\text{F}_3(\text{Si}_3\text{O}_9)) = 7.09$ eV which should be compared with the value of 7.24 eV derived from the observed Ce^{3+} centroid shift. For both compounds LaOBr and La$_3$F$_3$(Si$_3$O$_9$) we find a mismatch of about 0.15 eV demonstrating that these methods are less reliable.

4. Summary and conclusions

The U-value that determines the energy of the CTLs of Ln$^{4+/3+}$ and Ln$^{3+/2+}$ with respect to the vacuum level can be determined from experimental data provided that sufficient information is available on different lanthanides in the same compound with various experimental techniques. Depending on the quality of the data, it provides U-values with estimated ±0.15 eV accuracy. Already in [20,22] a relation between the U-value and the centroid shift of the Ce^{3+} 4f-5d transition energies was demonstrated as illustrated in Fig. 2 and expressed with Eq. (3). Centroid shifts can be determined with ±0.05eV accuracy and are known for 175 different inorganic compounds. This all provides good estimates for U_c. For most compounds the Ce^{3+} centroid shift is not known or just not possible to determine. The aim of this work was to find a good estimator for U for all types of different compounds. The estimator is based on the average electronegativity of the cations in the compounds as defined by Eq. (6) where the Pauling and corrected Pauling value for electronegativity are used as can be found in Fig. 3. For the oxides and fluorides, the U_c-values appear in bands of ± 0.1 eV width drawn in Fig. 4 and 5 which enables to estimate U_X with estimated ±0.1 eV accuracy. The expressions of Eq. (7) and (8) can be used. A slight improvement of accuracy can be made by taking the site size into account since for the same χ_{av} the U_c-value tends to be slightly smaller on small lattice sites as compared to large ones. For the Cl, Br, I, S, Se compounds there appears not much dependence on the value of χ_{av}. $U_c(A)$ is around 6.65-6.8 eV for chlorides, 6.5-6.6 eV for bromides, and 6.2-6.4 eV for iodides with a slight tendency that the relatively small Y^{3+}, Lu^{3+} and Ca^{2+} have relatively low U_c-value. The few data on sulfide and selenide compounds fall between 6.1-6.3 eV. The U_c-value for the subset of compounds with more than one type of anion in the composition are more difficult to estimate. One may treat those compounds as a 'mix' of compounds each with just one type of anion

and estimated U_w from the U of each compound in that 'mix'. Accuracy is then limited to 0.1-0.15 eV. With Eq. (3) the estimator for U can be converted to an estimator for ϵ_c, and one may therefore also predict the centroid shift from electronegativity values for numerous different inorganic compounds.

In constructing of VRBE schemes, it is adviced to start with the best estimate for the U-value with one of the above methods. The U-value can be adjusted slightly, say $\pm$ 0.1 eV, after adding all experimental data on energies that concern electron or hole transport from a lanthanide to either the CB or the VB to the diagram until best agreement is obtained. Note that an overall error of ± 0.1eV in U translates to an error of $\approx \mp 0.05$eV in the Ln$^{3+/2+}$ CTLs and $\approx \mp 0.15$eV in the Ln$^{4+,3+}$ CTLs. One may regard this as the limiting accuracy in lanthanide CTL energies with respect to the vacuum level. Of course there is also a systematic error present in Eq. (1) but that one will drop out when VRBE diagrams of different compounds are compared with each other.

CRediT authorship contribution statement

Pieter Dorenbos was responsible for all elements that led to this manuscript including conceptualization, writing, reviewing, editing, analysis of data, preparing of figures, literature research etc.

Declaration of competing interest

The authors declare that they have no known competing financial interests or personal relationships that could have appeared to influence the work reported in this paper.

Data availability

No data was used for the research described in the article.

References

[1] P. Dorenbos, Chem. Mater. 17 (2005) 6452.
[2] A.J.J. Bos, Radiat. Meas. 41 (2007) S45.
[3] P. Dorenbos, J. Mater. Chem. C 11 (2023) 8129.
[4] A. Trovarelli, Catal. Rev. Sci. Eng. 38 (1996) 439.
[5] D.S. McClure, C. Pedrini, J. Phys. Colloq. 46 (C7) (1985) 397.
[6] C. Pedrini, F. Rogemond, D.S. McClure, J. Appl. Phys. 59 (1986) 1196.
[7] C.W. Thiel, H. Cruguel, H. Wu, Y. Sun, G.J. Lapeyre, R.L. Cone, R.W. Equall, R.M. Macfarlane, Phys. Rev. B 64 (2001) 085107.
[8] C.W. Thiel, R.L. Cone, J. Lumin. 131 (2011) 386.
[9] D.S. Hamilton, S.K. Gayen, G.J. Pogatshnik, R.D. Ghen, W.J. Miniscalco, Phys. Rev. B 39 (1989) 8807.
[10] J.K. Lawson, S.A. Payne, J. Opt. Soc. Am. B 8 (1991) 1404.
[11] W.M. Yen, M. Raukas, S.A. Basun, W. van Schaik, U. Happek, J. Lumin. 69 (1996) 287.
[12] U. Happek, S.A. Basun, J. Choi, J.K. Krebs, M. Raukas, J. Alloys Compd. 303 (2000) 198.
[13] P. Dorenbos, J. Phys. Condens. Matter 15 (2003) 8417.
[14] A. Lecointre, A. Bessiere, A.J.J. Bos, P. Dorenbos, B. Viana, S. Jacquart, J. Phys. Chem. C 115 (2011) 4217.
[15] P. Dorenbos, Opt. Mater. 69 (2017) 8.
[16] P. Dorenbos, Phys. Rev. B 85 (2012) 165107.
[17] P. Dorenbos, Phys. Rev. B 87 (2013) 035118.
[18] P. Dorenbos, J. Lumin. 214 (2019) 116536.
[19] P. Dorenbos, J. Lumin. 222 (2020) 117164.
[20] P. Dorenbos, J. Lumin. 136 (2013) 122.
[21] P. Dorenbos, Phys. Rev. B 65 (2002) 235110.
[22] P. Dorenbos, J. Lumin. 135 (2013) 93.
[23] P. Dorenbos, Phys. Rev. B 62 (2000) 15640.
[24] P. Dorenbos, Phys. Rev. B 62 (2000) 15650.
[25] R.D. Shannon, Acta Crystallogr., Sect. A Cryst. Phys. Diffr. Theor. Gen. Crystallogr. 32 (1976) 751.
[26] Ting Wang, Zhiguo Xia, Qianchuan Xiang, Shiqiang Qin, Quanlin Liu, J. Lumin. 166 (2015) 106.
[27] J. Malito, Chim. Oggi-Chem. Today 13 (1995) 57.
[28] A.L. Allred, J. Inorg. Nucl. Chem. 17 (1961) 215.
[29] L. Pauling, The Nature of the Chemical Bond, Cornell University Press, New York, 1960.
[30] P.V. Kelsey Jr., J.J. Brown, J. Electrochem. Soc., Solid State Sci. Technol. 123 (1976) 1384.
[31] Jun-Lin Yuan, Hui Zhang, Jing-Tai Zhao, Hao-Hong Chen, Xin-Xin Yang, Guo-Bin Zhang, Opt. Mater. 30 (2008) 1369.
[32] A.M. Srivastava, S.J. Duclos, H.A. Comanzo, S.M. Loureiro, J.S. Vartuli, P.A. Schmidt, U. Happek, IEEE Trans. Nucl. Sci. 55 (2008) 1225.
[33] P. Dorenbos, J. Lumin. 105 (2003) 117.
[34] K. Shimamura, H. Sato, A. Bensalah, V. Sudesh, H. Machida, N. Sarukura, T. Fukuda, Cryst. Res. Technol. 36 (2001) 801.
[35] Y. Kubota, M. Tateno, H. Nishioka, K. Ueda, Rev. Laser Eng. 24 (1996) 353.
[36] V.X. Quang, N.N. Dat, V.P. Tuyen, N.M. Khaidukov, V.N. Makhov, L.D. Thanh, N.X. Ca, N.T. Thang, P.T.T. Nga, P.V. Do, Opt. Mater. 107 (2020) 110049.
[37] J.C. van't Spijker, P. Dorenbos, C.W.E. van Eijk, K. Kramer, H.U. Gudel, J. Lumin. 85 (1999) 1.
[38] E.V.D. van Loef, P. Dorenbos, C.W.E. van Eijk, K. Kramer, H.U. Gudel, Phys. Rev. B 68 (2003) 045108.
[39] G. Gundiah, K. Brennan, Z. Yan, E.C. Samulon, G. Wu, G.A. Bizarri, S.E. Derenzo, E.D. Bourret-Courchesne, J. Lumin. 149 (2014) 374.
[40] F. Patrick Doty, Xiaowang Zhou, Pin Yang, Mark A. Rodriguez, Sandia National Laboratories Albuquerque, New Mexico 87185 and Livermore, California 94550, Sandia Report SAND2012-9951, 2012.
[41] Qu Zeng, Hongbin Liang, Guobin Zhang, M. Danang Birowosuto, Zifeng Tian, Huihong Lin, Yibinb Fu, Pieter Dorenbos, Qiang Su, J. Phys. Condens. Matter 18 (2007) 9549.
[42] Irina V. Berezovskaya, Shihang Zhou, Bibo Lou, Min Yin, Chong-Geng Ma, Anatoliy S. Voloshinovskii, Vladimir P. Dotsenko, J. Lumin. 244 (2022) 118730.
[43] Chonggeng Guo, Lin Luan, Liang Shi, Hyo Jin Seo, Electrochem. Solid-State Lett. 13 (2010) J28.
[44] Xinmin Zhang, Boowon Park, Namsik Choi, Jongsu Kim, G.C. Kim, J.H. Yoo, Mater. Lett. 63 (2009) 700.
[45] Yanhua Song, Guang Jia, Mei Yang, Yeju Huang, Hongpeng You, Hongjie Zhang, Appl. Phys. Lett. 94 (2009) 091902.
[46] Lixin Ning, Cuicui Zhou, Wanping Chen, Yucheng Huang, Changkui Duan, Pieter Dorenbos, Ye Tao, Hongbin Liang, J. Phys. Chem. C 119 (2015) 6785.
[47] Youjun Kang, Ye Li, Jianhui Zhang, Shuaishuai Sun, Yan Huang, Ye Tao, Hongbin Liang, Qiang Su, J. Lumin. 143 (2013) 21.
[48] T. Shalapska, G. Stryganyuk, Yu Romanyshyn, D. Trots, P. Demchenko, A. Gektin, A. Voloshinovskii, P. Dorenbos, J. Phys. D, Appl. Phys. 43 (2010) 405404.
[49] P. Demchenko, A. Gektin, A. Krasnikov, I. Pashuk, T. Shalapska, G. Stryganyuk, A. Voloshinovskii, S. Zazubovich, J. Phys. D, Appl. Phys. 46 (2013) 235103.
[50] A. Mayolet, Etude des processus d'absorption et de transfert d'energie au sein de materiaux inorganiques luminescents dans le domaine UV et VUV, thesis, Universite de Paris XI Orsay, 1995.
[51] P. Dorenbos, Unpublished data measured at 10 K at DESY, Hamburg.
[52] Rui Shi, Lixin Ning, Zhiqiang Wang, Jiatang Chen, Tsun-Kong Sham, Yan Huang, Zeming Qi, Cuijin Li, Qiang Tang, Hongbin Liang, Adv. Opt. Mater. 7 (2019) 1901187.
[53] Jin He, Rui Shi, Zhiqiang Wang, Minsi Li, Tsun-Kong Sham, Lianshe Fu, Adv. Opt. Mater. (2021) 2101751.
[54] Rongfu Zhou, Litian Lin, Chunmeng Liu, Pieter Dorenbos, Ye Tao, Yan Huang, Hongbin Liang, Dalton Trans. 47 (2018) 306.
[55] B. Finke, L. Schwarz, P. Gurtler, M. Kraas, M. Joppien, J. Becker, J. Lumin. 60&61 (1994) 975.
[56] Yiyi Ou, Weijie Zhou, Pieter Dorenbos, Hongbin Liang, Inorg. Chem. 62 (2023) 6181.
[57] Feng Zhang, Yuhua Wang, Yan Wen, Dan Wang, Ye Tao, Opt. Mater. 33 (2011) 475.
[58] Chien-Hao Huang, Teng-Ming Chen, Bing-Ming Cheng, Inorg. Chem. 50 (2011) 6552.
[59] Fang Su, Bibo Lou, Yiyi Ou, Yunlin Yang, Weijie Zhou, Chang-Kui Duan, Hongbin Liang, J. Phys. Chem. C 125 (2021) 595.
[60] Donghao Wen, Quanfeng Li, Yiyi Ou, Yunlin Yang, Zeming Qi, Pieter Dorenbos, Hongbin Liang, Dalton Trans. 51 (2022) 17809.
[61] Rui Shi, Yan Huang, Ye Tao, Pieter Dorenbos, Haiyong Ni, Hongbin Liang, Inorg. Chem. 57 (2018) 8414.
[62] Rui Shi, Xiaojun Wang, Yan Huang, Ye Tao, Lirong Zheng, Hongbin Liang, J. Phys. Chem. C 122 (2018) 7421.
[63] Jiangqing Wang, Weiren Zhao, Jianming Zhong, Licai Lan, J. Mater. Sci., Mater. Electron. 25 (2014) 2162.
[64] Jianqing Wang, Weiren Zhao, Luminescence (2016) 1–7.
[65] Kazuki Asami, Jumpei Ueda, Kotaro Yasuda, Kenta Hongo, Ryo Maezono, Mikhail G. Brik, Setsuhisa Tanabe, Opt. Mater. 84 (2018) 436.
[66] Litian Lin, Lixin Ning, Rongfu Zhou, Chunyan Jiang, Mingying Peng, Yucheng Huang, Jun Chen, Yan Huang, Ye Tao, Hongbin Liang, Inorg. Chem. 57 (2018) 7090.
[67] Mubiao Xie, Haiyin Su, Jiajun Chen, Opt. Mater. 88 (2019) 48.
[68] Rui Shi, Xiaoxiao Huang, Tiantian Liu, Litian Lin, Chunmeng Liu, Yan Huang, Lirong Zheng, Lixin Ning, Hongbin Liang, Inorg. Chem. 57 (2018) 1116.
[69] N. Kodama, M. Yamaga, B. Henderson, J. Appl. Phys. 84 (1998) 5820.
[70] N. Kodama, T. Takahashi, M. Yamaga, Y. Tanii, J. Qui, K. Hirau, Appl. Phys. Lett. 75 (1999) 1715.

[71] Litian Lin, Rui Shi, Rongfu Zhou, Qi Peng, Chunmeng Liu, Ye Tao, Yan Huang, Pieter Dorenbos, Hongbin Liang, Inorg. Chem. 56 (2017) 12476.

[72] G. Blasse, A. Bril, J. Chem. Phys. 47 (1967) 5139.

[73] E. van der Kolk, J.T.M. de Haas, A.J.J. Bos, C.W.E. van Eijk, P. Dorenbos, J. Appl. Phys. 101 (2007) 083703.

[74] Xionghui Zeng, Lianhan Zhang, Guangjun Zhao, Jun Xu, Yin Hang, Huiyong Pang, MingYin Jie, Chengfeng Yan, Xiaoming He, J. Cryst. Growth 271 (2004) 319.

[75] XiaoDan Wang, Tao Pan, TaoCheng Zang, JianKang Li, ZhiWei Zhao, LianHan Zhang, Jun Xu, Sci. China Ser. E, Tech. Sci. 52 (2009) 3678.

[76] Yu. Zorenko, V. Gorbenko, I. Konstankevych, B. Grinev, M. Globus, Nucl. Instrum. Methods A 486 (2002) 309.

[77] Yu.V. Zorenko, V.I. Gorbenko, G.B. Stryganyuk, V. Mikhailin, V.N. Kolobanov, D.A. Spasskii, K. Blazek, M. Nikl, Opt. Spectrosc. 99 (2005) 923.

[78] Xue-Jian Liu, Hui-Li Li, Rong-Jun Xie, Yi Zeng, Li-Ping Huang, J. Lumin. 124 (2007) 75.

[79] A. Zych, Luminescence properties of Ce3+, Pr3+, and Nd3+ activated scintillators for Positron Emission Tomography (PET), thesis, Utrecht University, 2011.

[80] S. Asano, N. Yamashita, Y. Ogawa, Phys. Status Solidi B 118 (1983) 89.

[81] Jianhui Zhang, Jing Wang, Ruijin Yu, Haibin Yuan, Qiang Su, Mater. Res. Bull. 44 (2009) 1093.

[82] Y.Q. Li, G. de With, H.I. Hintzen, J. Lumin. 116 (2006) 107.

[83] Y.Q. Li, N. Hirosaki, R.J. Xie, T. Takeda, M. Mitomo, Chem. Mater. 20 (2008) 6704.

[84] Z. Zhang, O.M. ten Kate, A. Delsing, E. van der Kolk, P.H.L. Notten, P. Dorenbos, J. Zhao, H.T. Hintzen, J. Mater. Chem. 22 (2012) 9813.